ORIGINAL ARTICLE

Neuropathologic damage induced by radiofrequency ablation at different temperatures - an experimental study

Yu Dong[1], Ying Chen[1], Baoguo Yao[1], Peng Song[1], Ruiting Xu[1], Rui Li[1], Ping Liu[1], Yu Zhang[1], Li Mu[1], Xin Tong[1], Linwei Ma[1], Jianjun Yu[1], Li Su[1*]

Biomedica - Official Journal of University of Health Sciences, Lahore, Pakistan
Volume 37(4):234-239
https://doi.org/10.51441/BioMedica/5-519

ABSTRACT

Background and Objective: Radiofrequency ablation (RFA) is a safe and less invasive technique that uses an electric current to damage nerve tissue to stop it from sending pain signals. This study was aimed to determine the molecular mechanism of neuropathologic damage induced by RFA at different temperatures.

Methods: A total of 36 Sprague Dawley rats were used as model with neuropathological injury. These rats were divided into six groups based on the temperature stimulation at 42°C, 47°C, 52°C, 57°C, 62°C, and 67°C. Conduction time, distance, and velocity were recorded after thermal injury. Hematoxylin and eosin staining was used to observe the histopathological changes of sciatic nerve. Neural ion channel proteins such as sodium voltage-gated channel alpha subunit 9 (SCN9A), sodium channel B3 subunit (SCN3B) and neurofascin (NFASC) expression in sciatic nerve tissue were detected detected by Western Blot.

Results: Nerve conduction velocity (NCV) gradually decreased with the increase in temperature and neuronal damage was seen at 67°C. H&E staining showed increased degeneration of neurons with an increase in temperature from 47°C to 67°C. SCN9A and SCN3B expression at 57°C, 62°C, and 67°C was much higher; however, NFASC expression was lower at same temperatures.

Conclusion: Neuropathological damage caused by RFA at different temperatures shows positive correlation with NCV. Heat transfer injury affects the expression of SCN9A, SCN3B, and NFASC in sciatic nerve tissue.

Keywords: Radiofrequency ablation, thermal damage, sciatic nerve, neuron, nerve conduction.

Received: 09 September 2021 **Revised date:** 14 October 2021 **Accepted:** 26 November 2021

Correspondence to: Li Su
*Department of Thyroid and Breast Surgery, People's Hospital of Ningxia Hui Autonomous Region, Yinchuan, China.
Email: csli0984@126.com
Full list of author information is available at the end of the article.

Introduction

Radiofrequency ablation (RFA) is a minimally invasive technique being developed in recent years. The main principle behind the thermal ablation is the constant vibration of ions in the tissues under the action of the current of the radiofrequency electrode, resulting in friction, and increasing the temperature around the tissues.[1] Thermal effect induced by RFA increases the temperature of tissue as the radio frequency current flows through it. However, after reaching a certain temperature, the water inside and outside the cell evaporates, and denatures cell protein to achieve the purpose of treatment.[2] Radiofrequency refers to the electromagnetic waves with a certain range frequency. At present, there is no clear dividing standard so, the frequency range of 200~750 kHz is often used in medical applications.[3,4] RFA now has been widely used in clinical therapy with good efficacy for certain diseases like liver and lung cancer.[5-7] However, the mechanisms of neurological disease and neuropathologic injury have not been reported.

Transfer of heat to the surrounding tissue during ablation of diseased tissue cause thermal damage of recurrent laryngeal nerve. In clinical practice, controlling the temperature to ensure complete ablation of the lesion without causing damage to the peripheral tissues and nerves is still a worth studying problem. This study was conducted to determine the molecular mechanism of neuropathologic damage induced by RFA at different temperatures. It is always important to clarify the "heat transfer damage effect"

of RFA in order to guide clinicians to control the clinical RFA threshold.

Methods

This randomized controlled experimental study was conducted at the Department of Thyroid and Breast Surgery, People's Hospital of Ningxia Hui Autonomous Region, China, from April to December 2020 after approval from the Institutional Ethical Review Committee. A total of 36 Sprague Dawley (SD) rats of both genders, 9 to 10 weeks old and weighing 250 to 350 g were obtained from the Animal Experiment Center of Ningxia Medical University, China. [Animal Use License: SCXK (Ningxia) 2020-00010]. These experimental rats were uniformly fed at (22 ± 2) °C, with 40%-50% relative humidity by the animal experiment center.

Rat anti human primary antibodies sodium voltage-gated channel alpha subunit 9 (SCN9A), sodium channel B3 subunit (SCN3B), neurofascin (NFASC) (1:500), horseradish peroxidase (HRP) labeled sheep anti-rat secondary antibody (1:5, 000), and Hematoxylin and Eosin (H&E) staining kit were purchased from Beyotime Biotechnology, China.

Rats were divided into six groups based on the temperature with six rats in each group. The group 1 (42°C), group 2 (47°C), group 3 (52°C), group 4 (57°C), group 5 (62°C), and group 6 (67°C) were segregated for temperature ranges. At the same time, a control group was set without temperature damage intervention. All animal experiments were carried out in accordance with the national regulations on medical animal experiments. After 1 week of adaptive feeding, 36 SD rats were randomly stimulated with self-made temperature injury probe for 10 seconds, and the temperature was recorded respectively.

Neuropathological injury model and conduction time

After anesthesia, the sciatic nerve of the hind limb was exposed by making a cut through the skin, and the visual field of the central segment of the sciatic nerve was seen by detaching piriformis muscle. The hind limbs of the rats were straightly extended in a longitudinal plane along the passage and direction of the sciatic nerve. The distance between the stimulus and the receiving probe was measured using a vernier caliper.

The nerve stimulation probe was placed at the efferent site of the sciatic nerve (sciatic notch). The signal was received at the sciatic nerve of the rat ipsilateral ankle joint with the receiving probe electrode. The reference electrode was placed between the nerve stimulation and the nerve receiving probe (1 cm away). The self-made temperature injury probe was connected with the thermostatic hot water and placed 1 cm away from the nerve stimulation probe. BL-420E data acquisition & analysis system was used to control and adjust the stimulus intensity repeatedly. The stimulus intensity was used as the stimulus threshold, and the time value after temperature damage was recorded.

Nerve conduction velocity (NCV)

NCV was calculated as following: NCV (cm/ms) = conduction distance / conduction time (CT).

Haematoxylin and eosin staining

The rats were sacrificed by general anesthesia, and damaged sciatic nerve tissue by labeled heat range was removed. The rats were fixed in the supine position on the operating table, and 1 cm incision was made along the direction of the sciatic nerve at the junction of the left gluteus and femoral nerve. The sciatic nerve was freed with the hand, and intercepted 5 mm above and below the injury for reserve. Then, the skin and muscles in the middle of the rat's back were cut longitudinally and stripped to expose the spine. The spinal cord located at L4-L5 was removed. Sciatic nerve tissue was washed with normal saline at 4°C and fixed with neutral formalin for 12 hours. Then, the tissue was processed to make blocks and slides. Staining was performed according to the procedure of H&E staining kit, and morphology of sciatic nerve was observed under microscope.

Western blot

About 20 µg of proteins was extracted from the heat damaged sciatic nerve tissue of each group of rats. These proteins were isolated by sodium dodecyl sulphate-polyacrylamide gel electrophoresis. Objective and internal proteins were transferred to Nitrocellulose (NC) membrane, then closed with 5% skimmed milk powder sealing fluid for 2 hours at room temperature. Rat anti human primary antibody (1:500), and rat anti human primary antibody β-actin (1:1000) were added and incubated at 4°C overnight. Tris-buffered saline was used to wash four times, then HRP labeled sheep anti rat secondary antibody (1:500) was added and incubated at 37°C for 1 hour. Color was developed with the electrochemiluminescent solution, protein bands were exposed by gel image analysis system, and images were photographed and quantitatively analyzed. The experiment was repeated three times.

Statistical analysis

The data were analyzed by using Statistical Package for the Social Sciences version 22.0 software. The quantitative variables were measured as mean ± standard deviation (SD). One-way analysis of variance was applied for three or more groups. $P < 0.05$ was set as statistically significant.

Results

The conduction time was noted as 0.27 ± 0.12, 0.32 ± 0.14, and 0.37 ± 0.11 ms, in controls and at 42°C and 47°C, respectively. Conduction time was shortest in control group but no statistical difference among the controls, group 1 and 2 was seen. However, the conduction time (0.48 ± 0.15 ms) at 52°C was lower than at 57°C (0.96 ± 0.23 ms) and 62°C (1.7 ± 0.20 ms). There were obvious differences in the conduction time of ablative groups as compared with control group. Moreover, the value of groups at 67°C could not be recorded, indicating the damaged neurons (Table 1).

The conduction distance between the stimulus and receiving probe measured by vernier caliper was 2.73 ± 0.36,2.64 ± 0.50, 2.69 ± 0.80, 2.70 ± 0.68, 2.8 ± 0.52 cm in controls, and first four (1-4) groups, respectively. However, the distance was shortened significantly to 1.5 ± 0.34 cm at 62°C. Moreover, at 67°C, the distance between the stimulus probe and the receiving probe could not be measured, indicating the damaged neurons

NCV was found as 11.28 ± 4.07, 8.99 ± 2.61, and 7.27 ± 0.01 cm/ms in controls and group 1 and 2, respectively. Statistically, no significant difference between the control and group 1 was seen. However, NCV (5.71 ± 0.38 cm/ms) was significantly lower at 52°C compared to 42°C, 47°C, and controls. When the temperature reached at 67°C, NCV could not be calculated because the time and distance were not recorded thus showing neuronal necrosis (Figure 1).

H&E staining showed that the nuclei of rat sciatic nerves were centered in controls and group 1. Degenerated neurons, increased intracellular vacuoles, and shrunken neuroplasm were seen in groups 2 to 6. In addition, destroyed neuronal structure, nuclear changes and coagulation necrosis occurred at 67°C (Figure 2).

SCN9A and SCN3B expressions at 57°C, 62°C, and 67°C were much higher than controls and in the groups below 57°C ($P < 0.05$) thus presenting a positive correlation with higher temperature. However, the expression of NFASC at 57°C, 62°C, and 67°C was lower than the other groups ($P<0.01$) (Figure 3).

Discussion

RFA is considered as a thermal damage caused by electric current passing through tissues.[8] RFA is characterized by increased local temperature, causing damage to the lipid bilayer of cell membrane followed by rupture and cell lysis.[9]

Nerve tissue has the lowest resistance and therefore more vulnerable to thermal damage. The pathological manifestations in peripheral nerve after electric burn are characterized by cell disintegration, axonal degeneration, nerve fiber swelling, and demyelination.[10] The changes in cell structure and function after RFA have been widely observed, but the changes of macromolecular functional proteins and their effects on cell function have not been studied. There are different kinds of neural ion channels including SCN9A a large molecular protein that undergoes thermal damage both structurally and functionally. In addition, nerve damage is gradually strengthened with the increase in temperature induced by voltage and electricity.[11]

SCN3B is up-regulated in the dorsal root ganglion during nerve damage.[12] A series of plasticity changes occur in each subunit of SCN3B ion channel in neuropathic pain.[13] If SCN3B expression is decreased throughout the body, other complications may appear. It has been found that SCN3B knockout mice show changes in the electrophysiological characteristics of the heart.[14] In the current study, higher expression of SCN3B protein with the increase in temperature was reported indicating neuropathological damage. Therefore, down-regulation of SCN9A and SCN3B expressions could inhibit the neuropathic response, such as nerve injury and nerve pain. This can be used as a potential target for treating neuropathic injury.

NFASC, a transmembrane protein and also an important glial cell adhesion molecule, expresses primarily at the peripheral and central myelin axon-like junctions.[15] NFASC is abundant in the adult central nervous system, especially in the cerebellum and peripheral nerves.[16,17] NFASC mutations have recently been associated with neurodevelopmental disorders. NFASC plays a key role in the development and function of the axon initial segment (AIS) and Ranvier nodes.[18,19] The main role of NFASC is to connect the extracellular matrix and the intracellular skeleton of glial cells and neurons.[20] In adult animals, chronic intrathecal injection of antibodies also leads to NFASC loss and changes in motor nerve conduction.[21] In the present study lower expression of NFASC protein was seen at higher temperatures. The loss of NFASC expression caused a barrier to the formation of the initial axons, resulting in significant ataxia and decreased nerve conduction rate. Moreover, NFASC also plays an important role in the formation of myelin sheath structures and post-injury repair.[22]

Table 1. *Conduction time at different temperatures.*

Group	NC	42°C	47°C	52°C	57°C	62°C	67°C
Time (ms)	0.27 ± 0.12	0.32 ± 0.14	0.37 ± 0.11	0.48 ± 0.15**	0.96 ± 0.23***	1.7 ± 0.20***	Unable to record

**P < 0.01, ***P < 0.001, compared with NC group.

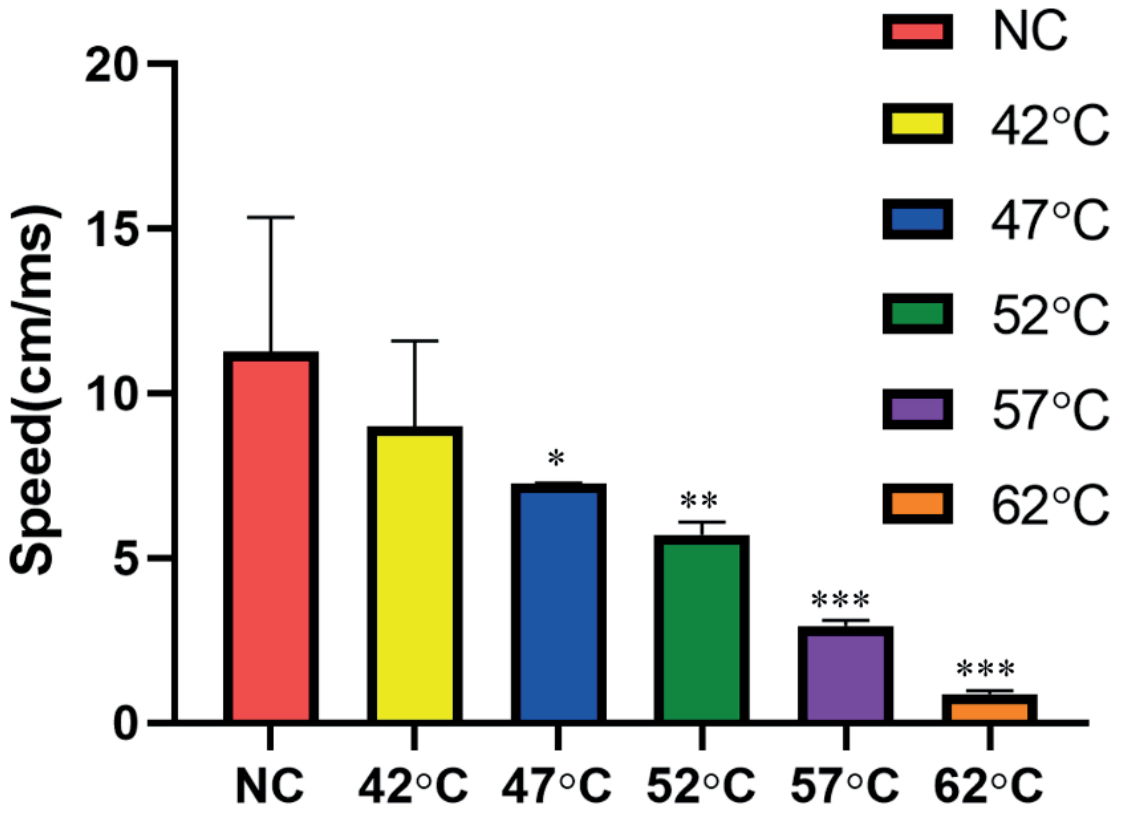

Figure 1. *Nerve conduction velocities in different temperature groups. (n = 3). ˙˙P < 0.01,˙˙˙P < 0.001 compared with NC group.*

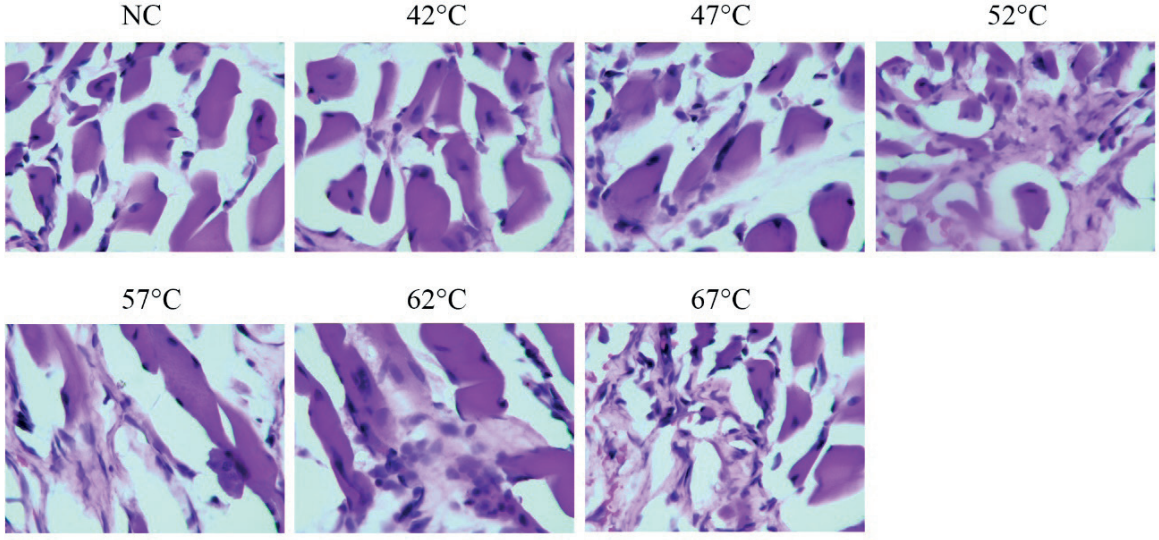

Figure 2. *H&E staining in sciatic nerve tissue in different groups (400×).*

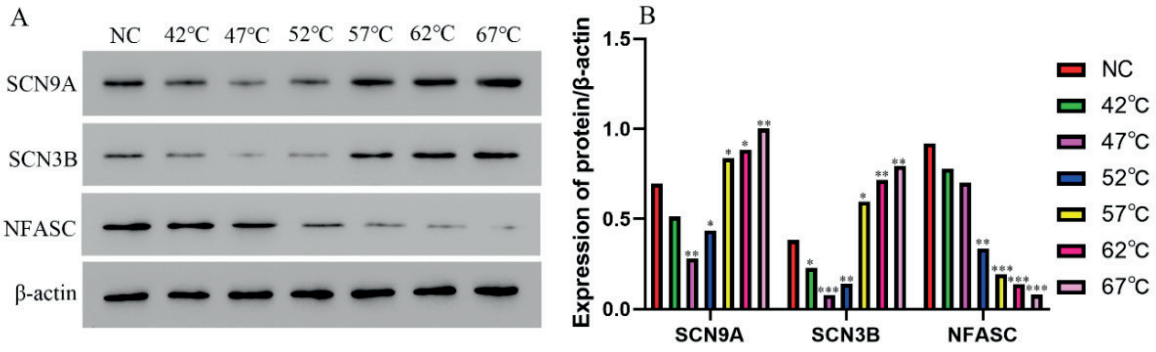

Figure 3. *Protein level of SCN9A, SCN3B, NFASC in different groups determined by the Western blotting (Mean ± SD, n = 3). A: Gray value; B: Statistical analysis. ¨P<0.01, ¨P<0.01,¨¨P<0.001 compared with control group.*

In the current study, neural damage is reported with the increase in temperature which is in accordance with the other study.[23] The mechanism behind the pain relief caused by radiofrequency current is destructive neural damage and the permanent impulses blockage through nerve pathways. Though excellent response can be achieved at low temperature with minimum neurodestructive effects. Therefore, it is recommended to avoid higher temperature because it may cause serious tissue damage with irreversible complications. Now -a -days certain guidance like three-dimensional CT or neuronavigator are used in order to improve the puncture precision and decrease the complications.[24]

Conclusion

Neuropathological damage caused by RFA at different temperatures is positively correlated with the NCV. Heat transfer injury affects the expression of SCN9A, SCN3B, and NFASC in sciatic nerve tissue.

Limitations of the study

The limitation in the study was adoption of the higher temperature ranges. Wide temperature ranges, including temperatures lower than 57°C could have been used in order to get more precise findings. Also, the histological parameters of the sciatic nerve could have been assessed with using special staining techniques. Future studies may be carried out incorporating these parameters.

Acknowledgement

The authors would like to express their sincere thanks to the staff at People's Hospital of Ningxia Hui Autonomous Region, Yinchuan, China for their technical help and support.

List of Abbreviations

G	Gram
H&E	Hematoxylin and eosin
HRP	Horseradish peroxidase
NC	Nitrocellulose
NCV	Nerve conduction velocity
NFASC	Neurofascin
RFA	Radiofrequency ablation
S	Seconds
SCN3B	Sodium channel B3 subunit
SCN9A	Sodium voltage-gated channel alpha subunit 9
SD	Sprague Dawley

Conflict of interest

None to declare.

Grant support and financial disclosure

This study was funded by the Northwest University for Nationalities, Central University of China vide Project No. 31920150055.

Ethical approval

This study was approved by the Ethical Review Board of People's Hospital of Ningxia Hui Autonomous Region, Yinchuan, China vide Project No. 31920150055, dated 12-03-2020.

Authors' contribution

YD, YC, BY, PS, LS: Conception and design, analysis and interpretation of data, drafting of manuscript.

RX, RL, PL, YZ, LM: Analysis and interpretation of data, revising the manuscript critically for important intellectual content.

XT, LM, JY: Analysis and interpretation of data

ALL AUTHORS: Approval of the final version of the manuscript to be published.

Authors' details

Yu Dong[1], Ying Chen[1], Baoguo Yao[1], Peng Song[1], Ruiting Xu[1], Rui Li[1], Ping Liu[1], Yu Zhang[1], Li Mu[1], Xin Tong[1], Linwei Ma[1], Jianjun Yu[1], Li Su[1]

1. Department of Thyroid and Breast Surgery, People's Hospital of Ningxia Hui Autonomous Region, Yinchuan, China

References

1. Pai M, Habib N, Senturk H, Lakhtakia S, Reddy N, Cicinnati VR, et al. Endoscopic ultrasound guided radiofrequency ablation, for pancreatic cystic neoplasms and neuroendocrine tumors. World J Gastrointest Surg. 2015;7(4):52–9. https://doi.org/10.4240/wjgs.v7.i4.52
2. Uche UI, Naidenko OV. Development of health-based exposure limits for radiofrequency radiation from wireless devices using a benchmark dose approach. Environ Health.

2021;20(1):84–7. https:// https://doi.org/10.1186/s12940-021-00768-1
3. Jung MY, Park JS, Lee JH. The principle and clinical application of radiofrequency devices in dermatology. Korean J Dermatol. 2013; 51(6):402–8.
4. Duncan DI, Kreindel M. Basic radiofrequency: physics and safety and application to aesthetic medicine. Aesthet Dermatol. Basel, Karger. 2015;2:1–22. https://doi.org/10.1159/000362747
5. Sahay A, Sahay N, Kapoor A, Kapoor J, Chatterjee A. Percutaneous image-guided radiofrequency ablation of tumors in inoperable patients-immediate complications and overall safety. Indian J Palliat Care. 2016; 22(1):67–73. https://doi.org/10.4103/0973-1075.173951
6. Cartier V, Boursier J, Lebigot J, Oberti F, Fouchard-Hubert I, Aubé C. Radiofrequency ablation of hepatocellular carcinoma: mono or multipolar? J Gastroenterol Hepatol. 2016 ;31(3):654–60. https:// https://doi.org/10.1111/jgh.13179
7. Hiraki T, Gobara H, Iguchi T, Fujiwara H, Matsui Y, Kanazawa S. Creation of an artificial hydromediastinum for radiofrequency ablation of lung tumor: a report of two cases. J Vasc Interv Radiol. 2014;25(11):1834–7. https://doi.org/10.1016/j.jvir.2014.03.035
8. Baxter CR. Present concepts in the management of major electrical injury. Surg Clin North Am. 1970;50(6):1401–18. https://doi.org/10.1016/s0039-6109(16)39297-0
9. Lee RC, Kolodney MS. Electrical injury mechanisms: electrical breakdown of cell membranes. Plast Reconstr Surg. 1987;80(5):672–9. https://doi.org/10.1097/00006534-198711000-00002
10. Delibas B, Kuruoglu E, Bereket MC, Onger ME. Allantoin, a purine metabolite, enhances peripheral nerve regeneration following sciatic nerve injury in rats: A stereological and immunohistochemical study. J Chem Neuroanat. 2021;117:102002. https://doi.org/10.1016/j.jchemneu.2021.102002
11. Han C, Hoeijmakers JG, Liu S, Gerrits MM, te Morsche RH, Lauria G, et al. Functional profiles of SCN9A variants in dorsal root ganglion neurons and superior cervical ganglion neurons correlate with autonomic symptoms in small fibre neuropathy. Brain. 2012;135(Pt 9):2613–28. https://doi.org/10.1093/brain/aws187
12. Shah BS, Stevens EB, Gonzalez MI, Bramwell S, Pinnock RD, Lee K, et al. Beta3, a novel auxiliary subunit for the voltage-gated sodium channel, is expressed preferentially in sensory neurons and is upregulated in the chronic constriction injury model of neuropathic pain. Eur J Neurosci. 2000;12(11):3985–90. https://doi.org/10.1046/j.1460-9568.2000.00294.x
13. Baron R, Binder A, Wasner G. Neuropathic pain: diagnosis, pathophysiological mechanisms, and treatment. Lancet Neurol. 2010;9(8):807–19. https://doi.org/10.1016/S1474-4422(10)70143-5
14. Hakim P, Brice N, Thresher R, Lawrence J, Zhang Y, Jackson AP, et al. Scn3b knockout mice exhibit abnormal sino-atrial and cardiac conduction properties. Acta Physiol (Oxf). 2010;198(1):47–59. https://doi.org/10.1111/j.1748-1716.2009.02048.x
15. Ango F, di Cristo G, Higashiyama H, Bennett V, Wu P, Huang ZJ. Ankyrin-based subcellular gradient of neurofascin, an immunoglobulin family protein, directs GABAergic innervation at purkinje axon initial segment. Cell. 2004;119(2):257–72. https://doi.org/10.1016/j.cell.2004.10.004
16. Thul PJ, Lindskog C. The human protein atlas: a spatial map of the human proteome. Protein Sci. 2018;27(1):233–44. https:// https://doi.org/10.1002/pro.3307
17. Carithers LJ, Moore HM. The genotype-tissue expression (GTEx) project. Biopreserv Biobank. 2015;13(5):307–8. https:// https://doi.org/10.1089/bio.2015.29031
18. Ghosh A, Sherman DL, Brophy PJ. The axonal cytoskeleton and the assembly of nodes of Ranvier. Neuroscientist. 2018;24(2):104–10. https://doi.org/10.1177/1073858417710897
19. Buttermore ED, Piochon C, Wallace ML, Philpot BD, Hansel C, Bhat MA. Pinceau organization in the cerebellum requires distinct functions of neurofascin in Purkinje and basket neurons during postnatal development. J Neurosci. 2012;32(14):4724–42. https://doi.org/10.1523/JNEUROSCI.5602-11.2012
20. Leshchyns'ka I, Sytnyk V. Reciprocal interactions between cell adhesion molecules of the immunoglobulin superfamily and the cytoskeleton in neurons. Front Cell Dev Biol. 2016;4(2):9–13. https://doi.org/10.3389/fcell.2016.00009
21. Manso C, Querol L, Lleixà C, Poncelet M, Mekaouche M, Vallat JM, et al. Anti-neurofascin-155 IgG4 antibodies prevent paranodal complex formation *in vivo*. J Clin Invest. 2019;129(6):2222–36. https:// https://doi.org/10.1172/JCI124694
22. Zou Y, Zhang WF, Liu HY, Li X, Zhang X, Ma XF, et al. Structure and function of the contactin-associated protein family in myelinated axons and their relationship with nerve diseases. Neural Regen Res. 2017;12(9):1551–8. https://doi.org/10.4103/1673-5374.215268
23. Choi S, Choi HJ, Cheong Y, Lim YJ, Park HK. Internal-specific morphological analysis of sciatic nerve fibers in a radiofrequency-induced animal neuropathic pain model. PLoS One. 2013;8(9):e73913. https:// https://doi.org/10.1371/journal.pone.0073913
24. Hong T, Ding Y, Yao P. Long-term efficacy and complications of radiofrequency thermocoagulation at different temperatures for the treatment of trigeminal neuralgia. Biochem Res Int. 2020;2020:1–10. https://doi.org/10.1155/2020/3854284